

Testing an array of 350 GHz drilled smoothwall horns using a vector near-field beam scanner

Paul K. Grimes^{1,*}, Edward Tong¹, Lingzhen Zeng¹, Jamie Leech² and Ghassan Yassin²

¹Smithsonian Astrophysical Observatory, Cambridge, MA, USA

²Oxford Astrophysics, University of Oxford, Oxford, UK

*Contact: pgrimes@cfa.harvard.edu, phone +1 (617) 496-7640

Abstract— We describe near-field tests and results of an 8 pixel close-packed feedhorn array that will be a key component of an 8 pixel prototype 350 GHz SIS mixer array receiver prototype under construction at SAO. We have fabricated an array of smoothwalled multiple flare angle feedhorns by direct drilling into a single block of aluminum. Testing of the feedhorns was carried out using a nearfield scanner and a vector network analyzer based on custom built transmitters and receivers and an HP vector voltmeter. The vector nearfield data is transformed to the farfield radiation pattern using Python code based on the NF2FF Matlab script[1].

I. INTRODUCTION

We are developing a multibeam SIS receiver for the 350 GHz band[2], consisting of 2x4 hexagonal packed receiver modules that will be mounted to the back of a large array of feedhorns. Each receiver module incorporates an 8-way LO splitter, cold LO injection, and 8 SIS mixers and associated hardware. By building the array from 8 pixel modules we can scale up the array receiver incrementally to at least 48 pixels.

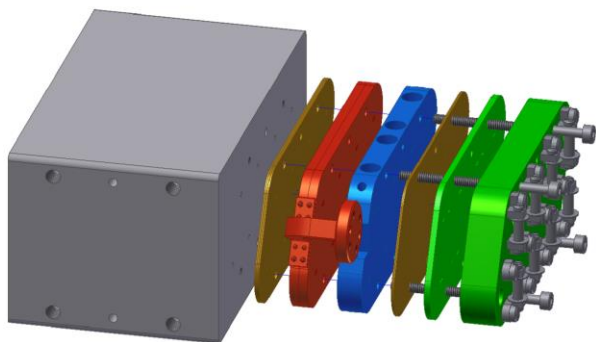


Figure 1. Exploded view of the multibeam array receiver module under development at SAO. The horn array (left, grey) serves as the main mechanical interface for the mixer module, which consists of (left to right): circular to rectangular waveguide transition (gold), LO splitter waveguide module (red), LO coupler module (blue), full- to half-height waveguide transition (gold), two part mixer module (green) with magnets and IF/bias ports.

For prototyping, a single receiver module will be mounted to the back of an 8 pixel array of smoothwall feedhorns designed and machined by Oxford Astrophysics[3] (Figure 1 and Figure 2). Each horn is made up of four conical sections

with variable flare angle and length, fed by a circular waveguide. The length of each section and the radii of each junction between sections is chosen using a genetic algorithm that matches the radiation pattern predicted by modal matching calculations of trial horn designs to the desired beam profile of the horn, and iterates towards a design that produces the desired beam pattern[4]. The optimized design of the feedhorns is shown in Figure 3.

The horn array is produced by drilling into a single aluminum block using a profiled D cutter that is made in the shape of the horn profile[5]. Each horn is separated from its neighbors by $\lambda/4$ at the center frequency of the design frequency band.

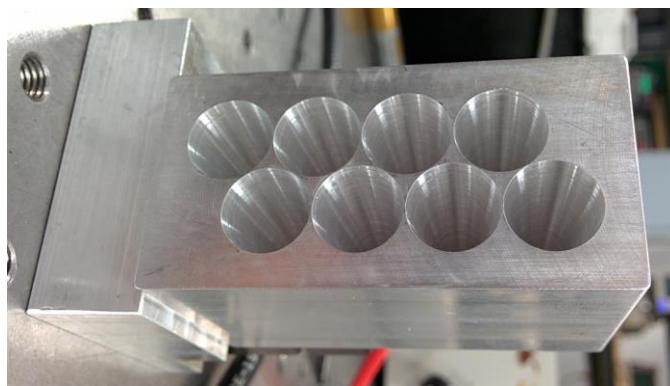


Figure 2. Photograph of drilled smoothwall horn array built by Oxford Astrophysics

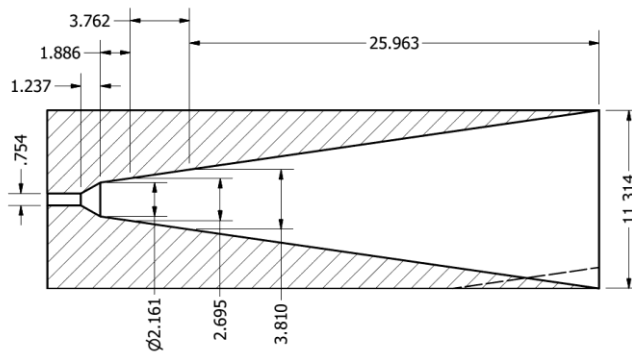


Figure 3. Profile of the feedhorn designed using a genetic algorithm in conjunction with modal-matching calculations. All dimensions are in mm.

In this paper we describe the tests that have been carried out in the SAO receiver laboratory to verify the performance of the horn array, using a nearfield scanning technique, which is then used to calculate the farfield radiation patterns of the horn under test.

The farfield radiation patterns provide a convenient measure of feedhorn performance, and are a useful tool for evaluating the match between the design and actual performance of the feedhorn by eye. However, direct measurement of the farfield pattern requires a relative large antenna test range, and involves significant signal losses due to the large distance between transmitter and receiver, which limits the dynamic range, particular at millimeter and submillimeter frequencies where transmitter power is limited.

Nearfield measurements can be carried out only a small distance between the transmitting antenna under test and an electrically small waveguide probe connected to the receiver. The waveguide probe is scanned on an x-y stage, to sample the complex tangential electric field produced by the transmitting antenna on a planar surface in front of the antenna. The farfield pattern is then calculated from the nearfield data by modal expansion of the field into plane waves[6]. This calculation is essentially a Fourier transform, and so can be carried out in a computationally efficient way.

II. NEARFIELD SCANNER

The SAO vector nearfield scanning system is built around a HP Vector Voltmeter which outputs the amplitude ratio and phase difference between its two input 3kHz to 300 MHz signals (Figure 4). Both input signals are downconverted from the mm-wave test signals by Pacific Millimeter harmonic mixers. The transmitter fundamental frequency is generated by a Agilent synthesizer at 1/12 the test frequency. The signal is multiplied into the W-band by an active tripler and the reference signal is tapped off in a cross-guide coupler where it is downconverted by a Pacific Millimeter harmonic mixer. The main signal is amplified by a W-band power amplifier to give sufficient power to drive a VDI doubler-doubler multiplier chain with an output power of up to 1 mW across the 330-373 GHz band.

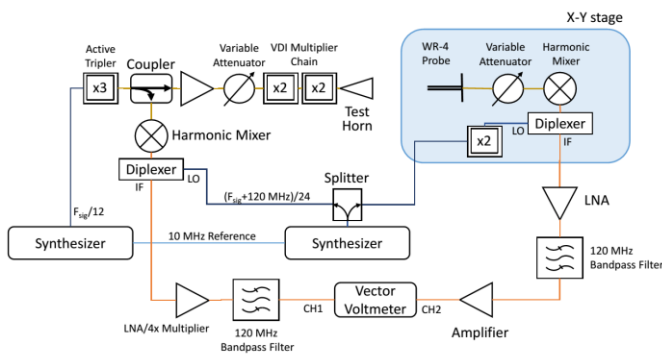


Figure 4. Vector nearfield scanner system diagram. Millimeter-wave signals are shown in gold, microwave LO signals in blue and IF signals in orange.

The receiver consists of a WR-4 waveguide probe, a variable attenuator to balance matching vs signal level and a Pacific Millimeter YMA harmonic mixer, mounted on a motorized X-Y stage. The LO signals for both the reference and receiver harmonic mixers are operated at the 24th (or 26th at the upper end of the band) harmonic, and driven by an HP synthesizer locked to the 10 MHz reference from the Agilen synthesizer. The 24th harmonic of the LO frequency is offset from the test signal frequency by 120 MHz. IF signals from both harmonic mixers are amplified by a series of room temperature LNAs and selected by 120 MHz bandpass filters. The IF signal from the reference harmonic mixer is multiplied by 4 by driving the reference IF LNA into saturation before bandpass filtering to take account of the x4 multiplication of the test signal that occurs after the reference signal is tapped off.

Rectangular Near Field: f = 345 GHz (z = 39 mm) - Copolar

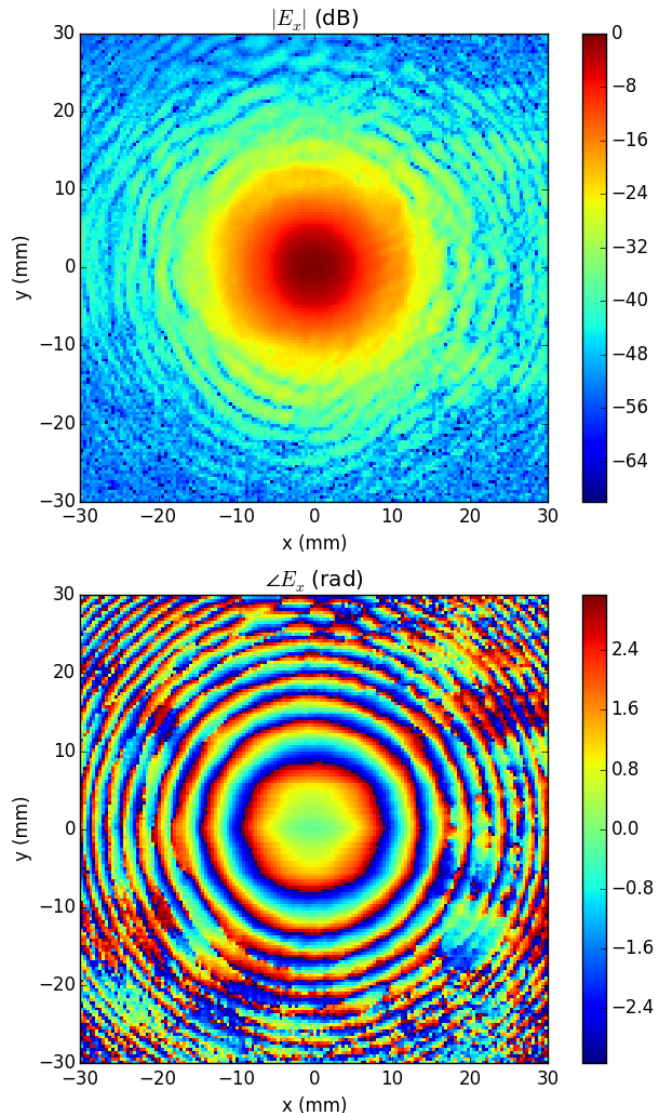


Figure 5. Typical nearfield scan results for the copolar amplitude (top) and phase (bottom). This scan was taken at a test frequency of 345 GHz.

The system typically achieves an amplitude signal to noise ratio of ~ 50 dB when the probe is at the center of the beam pattern of the smoothwall feedhorn. The phase stability is typically better than $\pm 3^\circ$ during a single line of the raster scan used to sample the nearfield beam pattern, but both the amplitude and phase drift on longer time scales. To mitigate this drift, at the middle of each line of the raster scan, the X-Y stage returns to the center reference position and records a new amplitude and phase reference. In postprocessing of scan data, these reference points are linearly interpolated and the drift subtracted.

Figure 5 shows typical nearfield data taken with the scanner, after calibration to remove the phase and amplitude drifts measured as described above. The amplitude dynamic range is slightly better than 50 dB at this frequency, and the phase noise is typically around $\pm 0.5^\circ$ at high signal power. Increased phase noise is evident in parts of the scan where the amplitude SNR is low. A complete nearfield scan takes just under 4 hours to complete.

III. FAR-FIELD PATTERNS

We have developed a Python script to carry out the transformation of the nearfield data into the farfield, based on the NF2FF Matlab script developed by Logan *et al*[1]. A description of the nearfield to farfield calculation can be found in Balanis' "Antenna Theory, Analysis and Design"[6].

In order to get high accuracy in the farfield patterns derived from nearfield data in the general case, the nearfield radiation pattern must be sampled at points no more than $\lambda/2$ apart (Nyquist criterion), and both co- and cross-polar fields must be measured out to large distances from the main beam, so that the nearfield pattern is not significantly truncated. In the case of a horn antenna with a relatively narrow beam and low cross-polarization, the cross-polar component of the nearfield pattern can be neglected. The narrow beam also means that the tangential electric field drops below the noise floor of the receiver relatively quickly, and so a large scan area is not required

The farfield patterns derived from the nearfield data can be compared to farfield patterns generated by the modal matching software used to design the horn profile. In Figure 6 we compare theoretical beam patterns calculated by the modal matching software for the nominal horn profile with the farfield patterns derived from nearfield measurements. The nearfield data used for these plots is measured on a 60 x 60 mm plane, 39 mm from the horn aperture, with a 0.4mm sample spacing in both x and y directions.

The measured patterns show very good agreement with the design predictions down to the -30 - -40 dB level in the near in sidelobes in the E-plane cuts. In the H-plane, the agreement is somewhat worse. This is most likely due to misalignment between the rectangular waveguide running from the multiplier chain to the horn array, which is held in position by a waveguide mounting clamp. A more careful alignment of the waveguide will be made for subsequent measurements of this and other horns. Overall, the farfield patterns indicate that the feedhorn itself is working well across the full frequency band of the multibeam receiver.

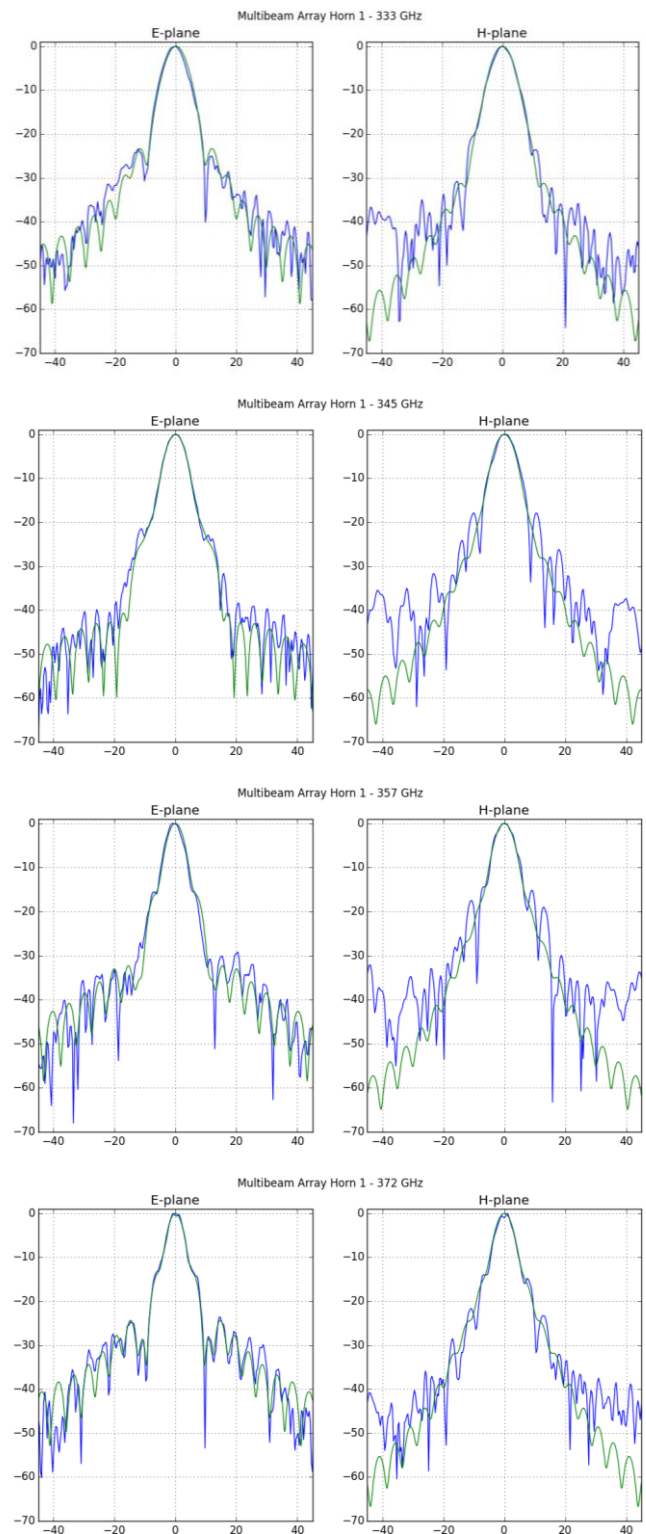


Figure 6. Farfield E- and H-plane radiation patterns for Horn 1 of the 8 pixel horn array derived from the nearfield scans (blue) compared with the E- and H-plane patterns predicted by the modal-matching calculation (green).

IV. CONCLUSIONS

We have built an 8-pixel close-packed feedhorn array by direct drilling of multiple flare angle smoothwall horns into a single block of aluminum. We have tested one horn from this array using a vector nearfield scanner, and developed data-analysis code to transform the nearfield data into farfield radiation patterns of the horn. We obtain good agreement between the farfield patterns and those predicted by the horn design software.

The feedhorn array will be a key component of a prototype multibeam SIS receiver array module that will form the basis of a larger array receiver instrument for the Greenland Telescope.

At the conference, we will present results from more extensive testing of the horn array across multiple pixels, and more details of the performance of the nearfield scanning system.

REFERENCES

- [1] J. Logan, A. P. Mynster, M. J. Pelk, C. Ponder, K. Van Caekenberghe, <http://nf2ff.sourceforge.net/> accessed Jan 2015.
- [2] Grimes, Paul K., et al. "Instrumentation for single-dish observations with the Greenland Telescope." *SPIE Astronomical Telescopes+ Instrumentation*. International Society for Optics and Photonics, 2014.
- [3] J. Leech , B. K. Tan , G. Yassin , P. Kittara , S. Wangsuya , J. Treuttel , M. Henry , M. L. Oldfield and P. G. Huggard "Multiple flare-angle horn feeds for sub-mm astronomy and cosmic microwave background experiments", *Astron. Astrophys.*, vol. 532, pp.A61 2011.
- [4] P. Kittara , A. Jiralucksanawong , G. Yassin , S. Wangsuya and J. Leech, "The design of potter horns for THz applications using a genetic algorithm", *Int. J. Infrared and Millimeter Waves*, vol. 28, no. 12, pp.1103-1114.
- [5] J. Leech , G. Yassin , B. K. Tan , M. Tacon , P. Kittara , A. Jiralucksanawong and W. S. "A new, simple method for fabricating high performance sub-mm focal plane arrays by direct machining using shaped drill bits", *Proc. 20th Int. Symp. Space Terahertz Technology*, pp.214 -218 2009.
- [6] Balanis, C.A. "Antenna Theory: Analysis and Design", Third edition, John Wiley & sons (2005).